Available online at www.sciencedirect.com

ScienceDirect

Physics Procedia 69 (2015) 464 – 471

Physics Procedia

10 World Conference on Neutron Radiography 5-10 October 2014

Neutron radiography of fluid flow for geothermal energy research

P. Bingham[a]*, Y. Polsky[a], L. Anovitz[a], J. Carmichael[a], H. Bilheux[a] D. Jacobsen[b], and D. Hussey[b]

[a]*Oak Ridge National Laboratory, Oak Ridge, TN 37831 USA*
[b]*National Insitute of Standards and Technology, Gaithersburg, MD 20899 USA*

Abstract

Enhanced geothermal systems seek to expand the potential for geothermal energy by engineering heat exchange systems within the earth. A neutron radiography imaging method has been developed for the study of fluid flow through rock under environmental conditions found in enhanced geothermal energy systems. For this method, a pressure vessel suitable for neutron radiography was designed and fabricated, modifications to imaging instrument setups were tested, multiple contrast agents were tested, and algorithms developed for tracking of flow. The method has shown success for tracking of single phase flow through a manufactured crack in a 3.81 cm (1.5 inch) diameter core within a pressure vessel capable of confinement up to 69 MPa (10,000 psi) using a particle tracking approach with bubbles of fluorocarbon-based fluid as the "particles" and imaging with 10 ms exposures.

Selection and peer-review under responsibility of Paul Scherrer Institut

Keywords: Geothermal Energy; Neutron Radiography

* Corresponding author. Tel.: +18655745680
E-mail address: binghampr@ornl.gov

Selection and peer-review under responsibility of Paul Scherrer Institut
doi:10.1016/j.phpro.2015.07.065

1. Introduction

Geothermal energy systems commonly in use today transport heat from the interior of the earth through the flow of water or brines through naturally fractured systems. This heat is either used directly for heating or used to generate electricity. These systems are limited to areas where three critical ingredients of heat, fluid, and permeability are all present. Efforts to expand geothermal energy to areas that do not naturally contain all three of these ingredients are currently in a research and development phase. These systems lack permeability and/or fluid and are called Enhanced Geothermal energy Systems (EGS). Development and commercialization of EGS requires understanding of fluid flow within fractures in geothermal rock under the pressures and temperatures ranging from 3 km to 10 km below the surface of the earth. A team of researchers from Oak Ridge National Laboratory (ORNL) has been working in conjunction with beam line scientists at imaging instruments at both the NIST Center for Neutron Research (NCNR) and ORNL to develop methods for imaging fluid flow in geological materials in an environmental chamber reproducing geothermal conditions.

Fluid flow measurement experiments commonly incorporate optically transparent materials to view two phase flow with visible light [Fourar et al, 1995 and Chen et al, 2004]. This is largely because the high light flux sources required for high speed image capture of the fluid motion are common. However, the transparency requirement for these methods is not suitable for either the geological samples of interest for EGS or the metallic pressure vessel materials needed to replicate EGS pressure and temperature conditions. Image based measurement methods applied to geologic measurements have been performed with x-ray radiography and computed tomography [Mees et al, 2003], neutron radiography [Jasti et al, (1992) and Deinart et al, 2002], PET [Goethals et al, 2009], and NMR [Fukushima, 1999]. Flow studies have focused on flow through porous media which is slow in comparison to forced flow through fractures in EGS. X-ray radiography has advantages over neutron radiography with respect to resolution and source strength. However, neutrons have a contrast advantages over x-rays for this application. Neutrons have a higher contrast between hydrogenous materials such as the fluids in a geothermal system and the high density and higher Z materials found in the geologic samples and in the surrounding environmental chamber.

With the low flux of neutron sources relative to x-ray and visible light sources, the challenge for imaging flow within a geothermal core lies in developing a method for high speed imaging that makes efficient use of the available neutrons. The following subsections describe the development of an environmental chamber and flow system, present the development and testing of forced flow imaging, and summarize performance for the flow imaging method.

2. Environmental Chamber and Flow System

A pressure vessel has been developed for neutron experiments that is capable of applying a radial confining pressure to a cylindrical rock core while independently supplying a pressurized flow in the axial direction [Polsky et al, 2013a]. Design goals for this chamber were to enable confinement pressures up to 69 MPa (10,000 psi), flow pressure up to 34.5 MPa (5,000 psi), and temperatures up to 350 °C using materials that minimize activation by the neutron beam. Figure 1 shows a picture of the vessel components and a schematic of the assembly. The sample core has a 38.1 mm diameter and can be up to 152.4 mm in length. A polyimide tube provides the isolation interface between the radial confinement pressure and the axial flow through the core. The geometry of the fluid passage within the components before and after the sample are matched to the sample fracture dimensions to minimize entrance and exit effects that would otherwise distort the flow field through the sample (item 2 in figure 1).

Material selection is key to the performance of the system for neutron experiments. Two vessel bodies have been produced with different materials (titanium and high strength aluminum). The titanium vessel meets both the pressure and temperature requirements listed earlier. The aluminum vessel meets the pressure requirements, but only at temperatures below 200 °C. The aluminum vessel is typically used for low temperature experiments, because it has a lower cross section for neutrons than titanium and produces better high speed radiographs by attenuating less of the neutron beam. Polyimide was selected for the sleeve based on its ability to withstand the required pressure differences and application temperatures using a thin layer that is relatively transparent to

neutrons. With the system assembled, the confinement pressure is applied to the core through a high pressure fitting in the side of the vessel body. Pressurized fluid is then applied to the flow entrance piece, passes through the core, and exits through the exit piece at the other end of the vessel. In addition to flow measurements, this chamber has also been used in measurement of strain in geologic cores in a neutron diffraction instrument [Polsky et al, 2013b].

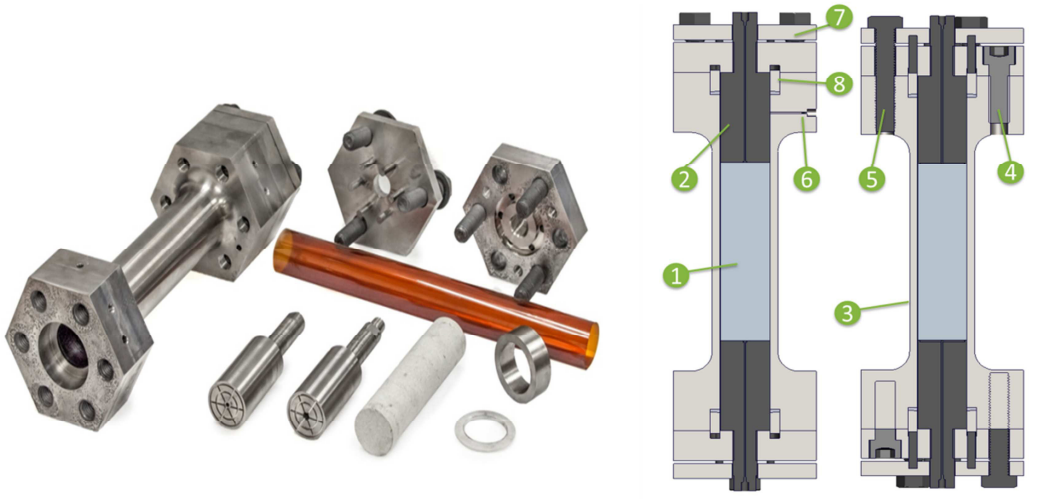

Figure 1. Chamber design (left) Picture of separated components (right) schematic (1)Geothermal core (2) flow entrance (or exit) piece (3) vessel body (4) internal retaining fasteners (5) seal forming fasteners (6) liner pressure port (7) seal forming plate assembly (8) seal area

3. Imaging Method Testing and Development

A series of imaging experiments has been performed in the development of flow imaging capabilities for geothermal samples under EGS conditions. Initial experiments concentrated on methods to generate contrast mechanisms for flow measurement. From those initial experiments, a particular experimental procedure was selected in which Fluorinert[†] bubbles are used to provide contrast and modifications were made to the imaging instrument to improve imaging statistics for higher speed flow. Finally, algorithms were developed to track the Fluorinert bubbles for quantification of flow patterns.

3.1. Development and testing of forced flow radiography

Using the chamber previously described, geologic cores were bisected through the center and shims fixed along the edges to produce an engineered rectangular fracture with a width of approximately 35 mm and thickness of 1.59 mm. A variable speed, positive displacement pump is used to control the rate of flow through the fractured core. The flow arrangement also contains a valve that allows insertion of a slug of contrast material into the chamber supply flow. In all of these radiography experiments, the neutron direction is perpendicular to the surface of the crack so that the image shows the 35 mm width of the crack with transmission through the crack thickness.

The system was first tested for high speed imaging of air/water interfaces. Figure 2 shows a series of image results containing an air/water interface and include a bubble propagating at a higher rate up through the water column. The images were created by subtracting an empty crack image to remove the core and chamber. High

[†] Certain trade names and company products are mentioned in the text or identified in an illustration in order to adequately specify the experimental procedure and equipment used. In no case does such identification imply recommendation or endorsement by the National Institute of Standards and Technology, nor does it imply that the products are necessarily the best available for the purpose.

contrast between air and water only required simple thresholds to identify boundaries as shown by lines in the figure. The images proceed from left to right with the water moving up through the crack. In this experiment, the environment was a 1.38 MPa (200 psi) confinement with 1 L/min flow of H_2O in the Ti chamber. The core was a Westerly Granite with a 1.59 mm thick crack. The data was captured at the NIST Neutron Imaging Facility (NIF) with a 150 μm thick ^{6}LiF/ZnS scintillator imaged by an Andor Neo sCMOS camera capturing 10 ms exposures at 14 Hz with 3x3 binning (145.5 μm pixels).

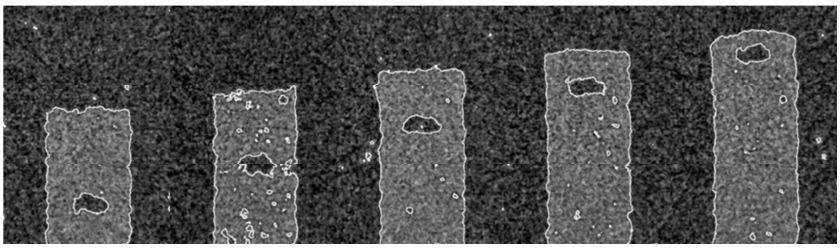

Figure 2. Air/Water interface experiment. Difference images show water flowing up through crack and bubble moving through water to catch the flow front.

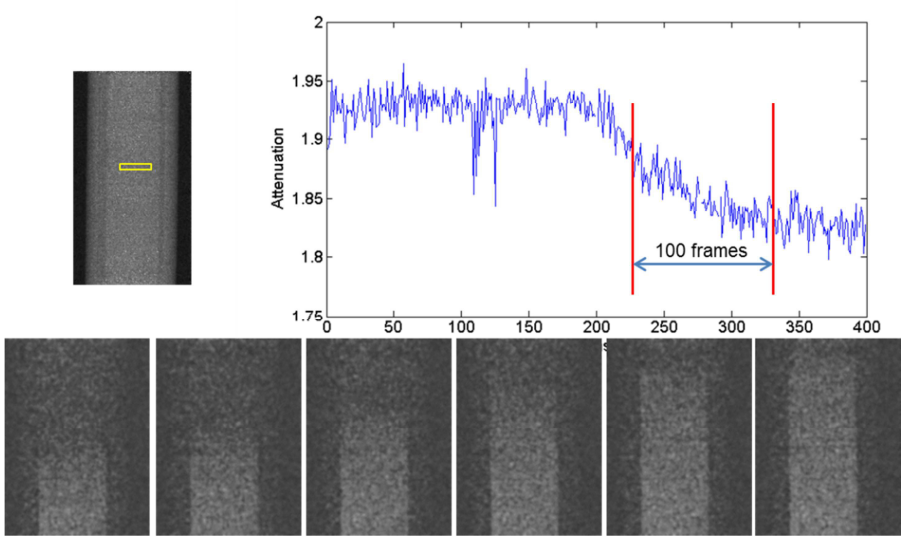

Figure 3. Liquid/liquid interface imaging. Borated H2O flow with D2O slug.

With the potential for flow imaging within the pressure vessel proven, experiments with various slugs of contrast agents were performed with a goal of capturing a liquid/liquid interface. These experiments employed various combinations of H_2O, Borated H_2O, and D_2O [Bingham et al, 2013]. For each of these experiments, mixing of the fluids prior to entering the fracture prevented capture of a clear interface. Figure 3 shows results from the highest contrast liquid/liquid interface experiment in which borated water was flowing through the system and a slug of D_2O was injected. For this experiment, the setup was the same as the previous air/water interface except the flow rate was dropped to 25 ml/min to reduce mixing and exposures were 20 ms at 10 Hz. The bottom row of images shows the flow of the D_2O slug into the borated H_2O filled crack with consecutive images 10 frames or 1 second apart. The graph shows the average attenuation in the box shown in the top left image versus time. While there is an obvious slope that could be used for front tracking through the flow in this example, this slope of this curve is low and results in significant flow velocity errors. Testing with higher flow rates resulted in increased mixing by the flow system which lowered the slope of the attenuation/time further.

Solid particle injection for particle tracking velocimetry was also attempted as an alternative to liquid contrast agent front tracking. Experiments with several particle types and sizes were performed. With the low resolution of the high speed imaging system, particles did not provide enough contrast unless they remained in clumps while passing through the crack. SiO2 beads provided some contrast, but not at a level needed for automated segmentation and tracking.

3.2. Instrument Reconfiguration

Based on the analysis of these previous experiments, it was determined that more neutrons were needed to improve the signal to noise ratio (SNR) for high speed flow measurements, and larger objects were needed for tracking flow in the crack. Modifications to the imaging system were made to improve the neutron flux and improve the SNR for the measurements. First, a high strength Al chamber was manufactured for improved transmission through the vessel. Using Al decreased the neutron cross section of the chamber by a factor of 20 over the Ti, but decreased the maximum operating temperature of the cell due to material strength reduction with temperature. Second, the typical imaging mode of the NIF was modified by moving the imaging stand 3 m closer to the reactor to increase the neutron flux by 4 times. Third, the 150 μm thick imager scintillator was replaced with a 300 μm thick scintillator for improved neutron detection efficiency. This increase in scintillator thickness comes at a sacrifice in resolution; however, this came as no cost to these experiments as the imager was already being binned to improve SNR. The left side of Figure 4 shows the modified imaging setup at the NIST NIF with the imager placed close to the front wall closest to the reactor.

In an effort to produce larger tracking centers, a search was made for liquids with low water solubility to prevent mixing. From this search, Fluorinert was selected. Fluorinert is a fluorocarbon-based fluid that does not mix with water. As a result, Fluorinert bubbles can be introduced into the flow stream and propagated through the crack. Fluorinert also has a cross section for neutrons that is about 0.02 that of H_2O so high contrast can be achieved between the two liquids. Figure 4 shows direct neutron radiographs of the Fluorinert bubbles flowing through the water filled crack. For this experiment, the same fluid flow system was used and a slug of Fluorinert introduced into the flow. Turbulence in this flow system broke the slug into a mass of bubbles propagating with the water. In these images, the flow is from top to bottom and time is left to right. The imaging environment was 1.38 MPa (200 psi) confinement pressure in the Al vessel and a 1.59 mm thick crack. Images were captured with 2x2 binning for 10 ms exposure time at a 30 Hz capture rate.

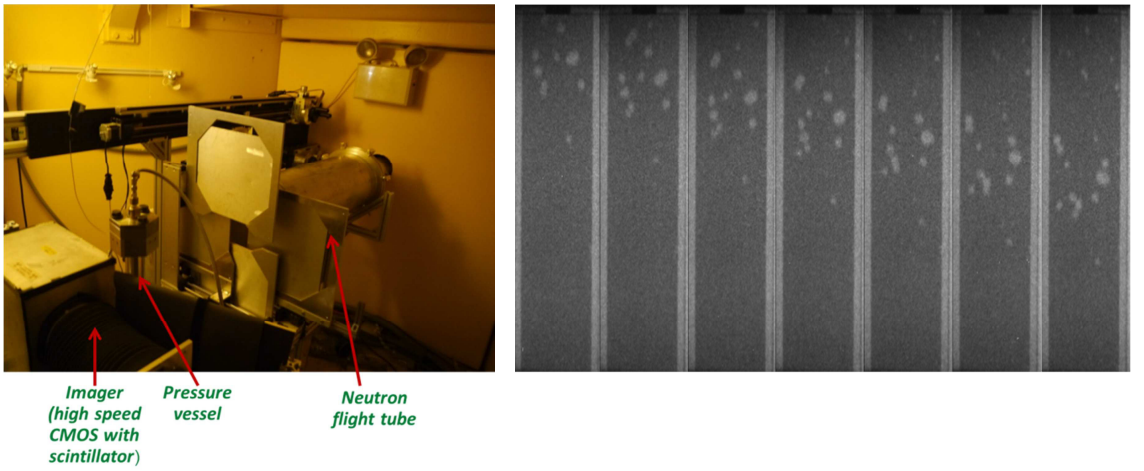

Figure 4. Fluorinert tracking experiment. (left) modified imaging setup at the NIF (right) Neutron radiographs of Fluorinert bubbles flowing through water filled crack.

3.3. Tracking Algorithm

The high contrast captured with the Fluorinert bubbles flowing through the H_20 filled crack allows segmentation of the individual bubbles and tracking of each bubble to quantify flow patterns through the crack. Typically in particle tracking experiments for flow measurement cross correlation methods are used on neighborhoods for tracking of particles. These methods are challenged by this data as the large motion between images requires a large correlation region that includes many other bubbles in the cluster and causes errors in the track. Therefore, a rule based tracking algorithm was developed to correlate positions of individual bubbles.

First, all of the time series images are normalized by subtracting a dark field image and dividing by an image in the flow measurement that does not contain any Fluorinert bubbles to remove the chamber and the core from the images. Second, segmentation is performed to calculate the position of each bubble in every frame. A threshold is selected to segment the bubbles from the water in each image and a dilation operation is used to remove internal voids and edge roughness of the segments. The centroid location, area, and image frame for each segmented bubble is stored in a list for the entire image series. Finally, a tracking algorithm attempts to link bubble positions through the time series. Challenges in tracking for this application include, large steps between images prevent simple image neighborhood correlations, clusters of bubbles cause confusion, bubbles occasionally stick along edges, and bubble interactions such as joining or splitting.

The tracking algorithm that has been implemented uses a probability approach based on rules to handle the challenges of the data set. Cycling frame by frame through the segmented bubble list, the distance between each bubble in the new frame and all tracks from the previous frame are calculated. Probability for a bubble in a new frame belonging to any of the current tracks is calculated using a binomial probability distribution function based on these distances. The function is binomial to account for moving and stuck bubbles. For stuck bubbles, a half Gaussian distribution is used to produce a probability density function peaked at 0 pixels shift between frames with a standard deviation of 10 pixels shift. For bubbles that are moving, a Gaussian centered at the previous bubble velocity with a standard deviation of 10 is calculated. The total probability density is a weighted sum of the still and moving distributions with the moving distribution weighted at 90 % and the still at 10 %. For startup of new tracks, the previous velocity is not known, so the user must enter an initial velocity estimate to be used by the tracking system. The tracking algorithm is quick, so we typically iterated on this value to produce good tracks. With probabilities for each bubble belonging to a previous track calculated for each frame, the algorithm iterates through the probability list assigning highest probability matches until all possible matches are assigned. In the current version of the algorithm, any track that is not matched to a bubble in the most recent frame is stopped and any bubble that is not assigned to a track starts a new track for the following frame. As such, any missed detection of a bubble in a frame will result in a break in the track. Longer tracks come from more reliable detections, so in analysis of flow fields a threshold is suggested to remove the more unreliable short tracks.

The tracking algorithm as described works well for image sets where bubbles are spread out in the frames. In these experiments clusters of bubbles resulted from flow method and occasionally a track would jump from one bubble to another. Inspection of these results showed that the displacement probability was working well, but did not limit direction. As a result, propagation in the opposite direction of flow or perpendicular to the flow was just as likely as propagation in the flow direction. Two rules were introduced to further restrict the tracks. Rule one was that probability for any track traveling against the flow direction is zero. Rule two required that the distance traveled by the bubble in the flow direction be at least two times greater than the distance traveled perpendicular to the flow.

Figure 5 shows two examples of tracking results from the algorithm. The images in this figure are both overlays of 20 consecutive images with bubbles flowing through. The overlay is a maximum overlay. Since the bubbles are bright in each frame, the bubbles from every frame appear in the overlay and give a visual display of the track. Bubbles are moving from right to left. Line overlays on these images depict the locations of calculated tracks. In the top image, an end to end track is shown along with two separate tracks calculated for a bubble that experienced a split after encountering a stuck bubble. This example was selected for clarity of the image, but typically the bubbles are smaller which lowers contrast and come in clusters. The bottom image shows tracks calculated from a cluster of smaller bubbles moving through the crack. In this example, several short tracks are seen resulting from breaks due to poor detection of the smaller bubbles, and a couple of tracks still jump to another

bubble due to clustering and also result in shortened tracks. With the current data, a threshold on track length (in frames) is used to remove these tracking errors. Further improvement of the imaging system to control bubble size and distribution is needed to improve tracking results due to clusters and poor detections as well as avoid errors in flow calculations due to bubble interactions.

4. Summary

Imaging of flow through a geological core within a metallic pressure vessel has been demonstrated using Fluorinert bubbles in water, and a tracking algorithm capable of isolating and tracking individual bubble tracks has been developed and tested on Fluorinert bubble flow data captured at the NIST NIF. As a next step, the flow system has been modified to include a needle bubbler that will be tested for further control of the Fluorinert introduction to the flow. This bubbler is expected to control bubble size and distribution to remove flow calculation errors related to bubble size and bubble interactions. With this new bubbler, flow experiments are planned to ramp up the flow rate and image flow pattern changes resulting from transition to the turbulent flow regime. While the current method is useful for verification of flow models, measurements will be more applicable if the contrast agent (Flourinert) is closer in density to that of water, so future efforts will also search for additional contrast agents.

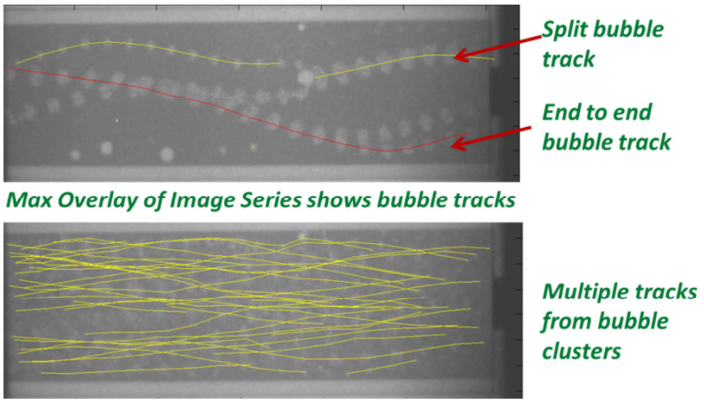

Figure 5. Fluorinert bubble tracking results

Acknowledgements

Research supported by the National Institute of Standards and Technology, U.S. Department of Commerce, in providing neutron research facilities used in this work.

A portion of this research was performed at the High Flux Isotope Reactor which is sponsored by the Scientific User Facilities Division, Office of Basic Energy Science, U.S. Department of Energy.

References

Bingham, P., Polsky, Y., and Anovitz, L., (2013), “Neutron imaging for geothermal energy systems,” SPIE Electronic Imaging 2013, Machine Vision Applications VI, March 6, 2013.

Chen C.Y., Horne, R.N. and Fourar, M. (2004), “Experimental Study of Liquid-Gas Flow Structure Effects on Relative Permeabilities in a Fracture” Water Resources Research, 40, W08301.

Deinart, M.R., Parlange, J.Y., Steenhuis, T., Throop, J., Unlu, K. and Cady, K.B. (2002), “Measurement of Fluid Contents and Wetting Front Profiles by Real-Time Neutron Radiography”, Journal of Hydrology, 290 (3-4), pp. 192-201.

Fourar, M., and S. Bories (1995), “Experimental Study of Air-Water Two Phase Flow Through a Fracture (Narrow Channel)”, Int. J. Multiphase Flow, 21, pp. 621– 637.

Fukushima, E., “Nuclear Magnetic Resonance as a Tool to Study Flow” (1999), Annu. Rev. Fluid Mech., 31, pp. 95-123.

Goethals, P, Volkaert, A, Jacobs, P, Roels, S and Carmeliet J, "Comparison of positron emission tomography and X-ray radiography for studies of physical processes in sandstone", (2009), Engineering Geology, 103(3-4), p.134-138.

Jasti, J.K. and Fogler, H.S. (1992), “Application of Neutron Radiography to Image Flow Phenomena in Porous Media”, AIChE Journal, 28 (4), pp.481 – 488.

Mees, F., Swennen, .R., Van Geet, M. and Jacobs, P. (2003), "Applications of X-Ray Computed Tomography in the Geosciences", Geological Society, London, Special Publications, 215, p. 1-6.

Polsky, Y., Anovitz, L., Bingham, P., and Carmichael, J., (2013), "Application of Neutron Imaging to Investigate Flow Through Fractures for EGS," Proceedings of the 38th Workshop on Geothermal Reservoir Engineering, Stanford University, Stanford, CA, February 11-13, 2013.

Polsky, Y., Dessieux, L., An, K., Anovitz, L., Bingham, P., and Carmichael, J. (2013) "Development of a neutron diffraction based experimental capability for investigating hydraulic fracturing for EGS-like conditions," Thirty-Eighth Workshop on Geothermal Reservoir Engineering, Stanford, CA.